

# Black-Box Optimization for Automated Discovery

Published as part of the Accounts of Chemical Research special issue "Data Science Meets Chemistry".

Kei Terayama, Masato Sumita, Ryo Tamura, and Koji Tsuda\*



Cite This: *Acc. Chem. Res.* 2021, 54, 1334–1346



Read Online

ACCESS |

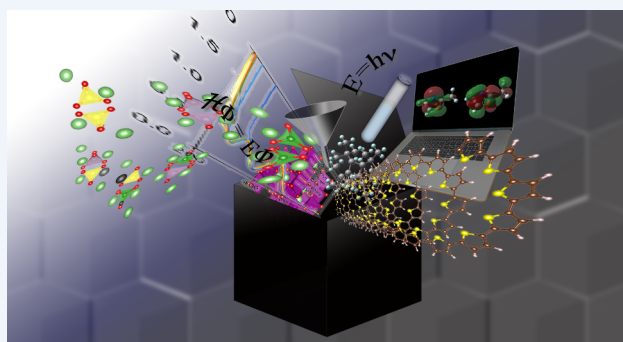
Metrics & More

Article Recommendations

**CONSPECTUS:** In chemistry and materials science, researchers and engineers discover, design, and optimize chemical compounds or materials with their professional knowledge and techniques. At the highest level of abstraction, this process is formulated as black-box optimization. For instance, the trial-and-error process of synthesizing various molecules for better material properties can be regarded as optimizing a black-box function describing the relation between a chemical formula and its properties. Various black-box optimization algorithms have been developed in the machine learning and statistics communities. Recently, a number of researchers have reported successful applications of such algorithms to chemistry. They include the design of photofunctional molecules and medical drugs, optimization of thermal emission materials and high Li-ion conductive solid electrolytes, and discovery of a new phase in inorganic thin films for solar cells.

There are a wide variety of algorithms available for black-box optimization, such as Bayesian optimization, reinforcement learning, and active learning. Practitioners need to select an appropriate algorithm or, in some cases, develop novel algorithms to meet their demands. It is also necessary to determine how to best combine machine learning techniques with quantum mechanics- and molecular mechanics-based simulations, and experiments. In this Account, we give an overview of recent studies regarding automated discovery, design, and optimization based on black-box optimization. The Account covers the following algorithms: Bayesian optimization to optimize the chemical or physical properties, an optimization method using a quantum annealer, best-arm identification, gray-box optimization, and reinforcement learning. In addition, we introduce active learning and boundless objective-free exploration, which may not fall into the category of black-box optimization.

Data quality and quantity are key for the success of these automated discovery techniques. As laboratory automation and robotics are put forward, automated discovery algorithms would be able to match human performance at least in some domains in the near future.



## KEY REFERENCES

- Ju, S.; Shiga, T.; Feng, L.; Hou, Z.; Tsuda, K.; Shiomi, J. Designing Nanostructures for Phonon Transport via Bayesian Optimization. *Phys. Rev. X* 2017, 7, 021024.<sup>1</sup> *The combination of Bayesian optimization and atomistic Green's function enabled the automatic design of interfacial thermal conductance composed of Si and Ge, with only a few percent of the total candidate calculations.*
- Sumita, M.; Yang, X.; Ishihara, S.; Tamura, R.; Tsuda, K. Hunting for Organic Molecules with Artificial Intelligence: Molecules Optimized for Desired Excitation Energies. *ACS Cent. Sci.* 2018, 4, 1126–1133.<sup>2</sup> *We showed that a molecule generator based on Monte Carlo tree search is capable of designing photofunctional molecules through automatic design on a computer coupled with quantum chemical calculations and experimental synthesis of the designed molecules.*
- Terayama, K.; Tamura, R.; Nose, Y.; Hiramatsu, H.; Hosono, H.; Okuno, Y.; Tsuda, K. Efficient construction method for phase diagrams using uncertainty sampling. *Phys. Rev. Materials* 2019, 3, 033802.<sup>3</sup> *For materials design, the concept of active learning is used to efficiently and automatically construct phase diagrams while discovering new phases.*
- Terayama, K.; Sumita, M.; Tamura, R.; Payne, D. T.; Chahal, M. K.; Ishihara, S.; Tsuda, K. Pushing property limits in materials discovery via boundless objective-free

Received: October 30, 2020

Published: February 26, 2021



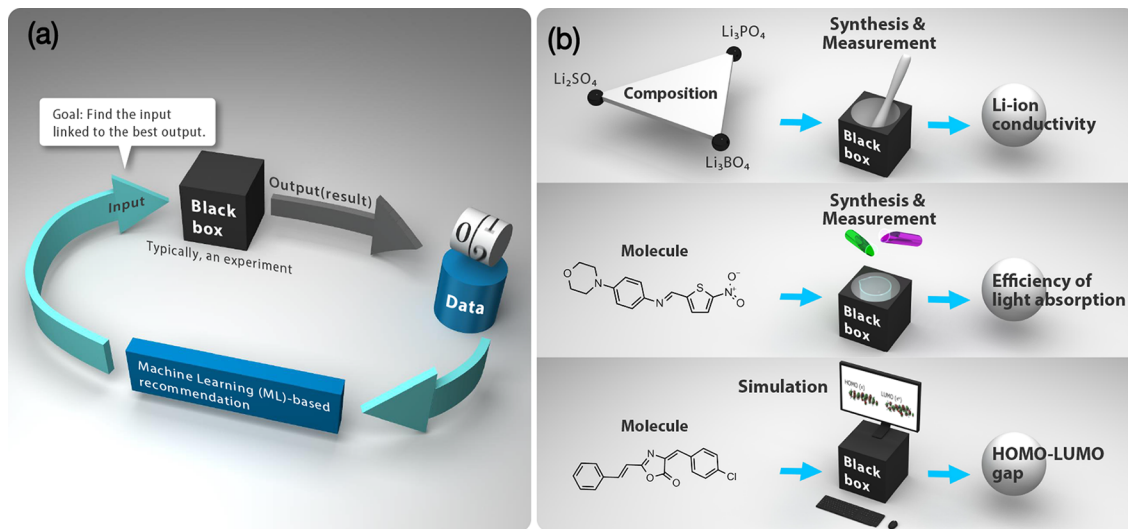


**Figure 1.** (a) Black-box optimization. For optimization, an ML-based algorithm recommends the next input from existing data. By evaluating the black box for the recommended input, the number of data points is increased by one. This process is repeated as much as necessary. (b) Examples of black-box functions in chemistry. In the first two examples, synthesis and measurement are regarded as black-box functions. A quantum chemical simulator can also be considered as a black-box function as shown in the last example.

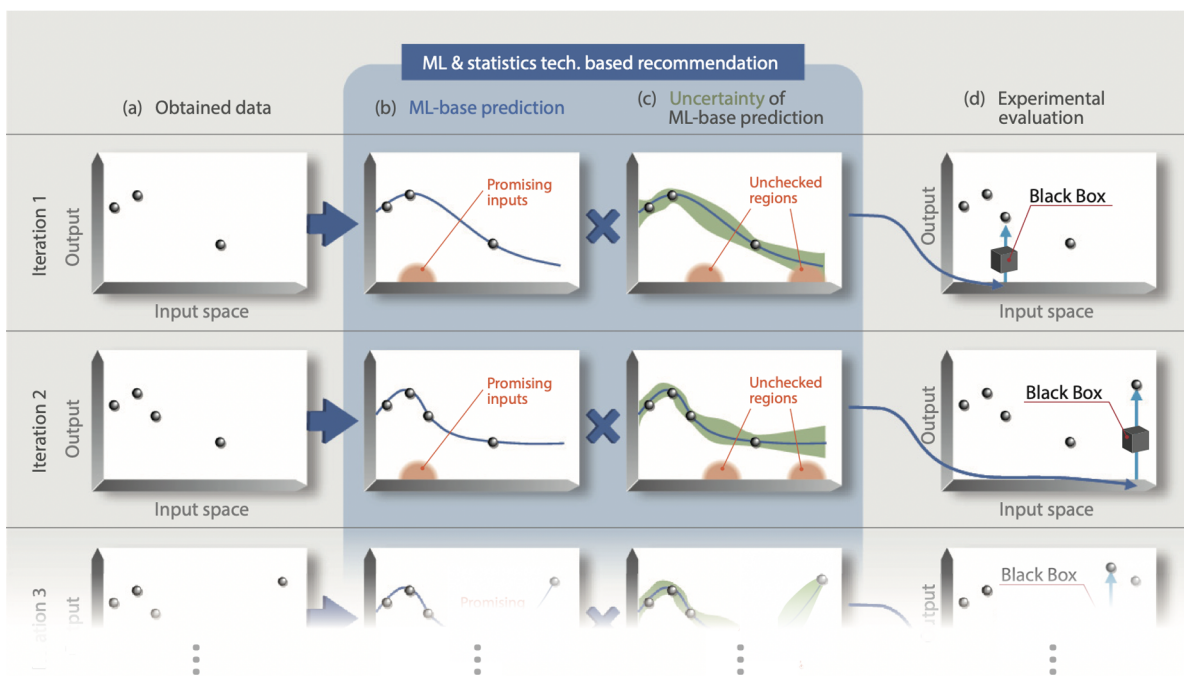


**Figure 2.** Role of uncertainty in black-box optimization. (a) Obtained input–output data. (b) Predicted output based on ML (blue line). Inputs in the orange region would be promising. (c) Degree of uncertainty of ML-based prediction (green regions). In the orange regions, inputs were not evaluated. (d) Next input recommended from the combination of panels b and c and its output of the black-box function evaluated. By repeating processes a–d, better inputs are discovered.

exploration. *Chem. Sci.* 2020, 11, 5959–5968.<sup>4</sup> The proposed method, BLOX, provides an efficient search for “out-of-trend” materials. It is demonstrated through simulations and experiments on light-absorbing molecules.

## 1. INTRODUCTION

### 1.1. Black-Box Functions in Chemistry and Materials Science

In decades past, designing products with a mathematical model has been a common subject of engineering research.<sup>5</sup> In fields

such as automotive and semiconductor engineering, a well-defined measure of product quality is often available, and the parameters of the product (such as size and shape) must be optimized for the best quality. The process of manufacturing a product and measuring its quality can be considered as a function, where the inputs are the parameter values and the output is the quality. Obviously, its analytical formula is unknown, but the evaluation is possible via manufacturing and measurement. Such a function is customarily called a *black-box function*.

By evaluating the black-box function with different inputs, a data set about an input–output relationship can be obtained. In a typical process of iterative black-box optimization shown in Figure 1a, a machine learning (ML) algorithm is employed for recommending a new input based on existing data. By evaluating the function at the recommended input, we obtain a new data point. In the next iteration, a new recommendation for input is obtained according to the updated data set. This process is repeated until the predetermined budget is met or a product of sufficiently high quality is obtained. When the ML algorithm works well, one can minimize the number of expensive function evaluations.

Scientific endeavor of designing new molecules and materials is far more complex than simply addressing the aforementioned engineering problems. Nevertheless, a number of researchers including ourselves found it useful and created a handful of successful case studies. Such a study starts with setting up a black-box function and identifying its input and output as in Figure 1b. In a study about optimizing Li-ion conductivity of solid electrolyte, the input is a composition ratio of materials and the output is the Li-ion conductivity. To discover candidate molecules useful in dye-sensitized solar cells, one can designate the black-box function as an experiment to measure the efficiency of light absorption of a molecule. In addition, it is common to treat quantum chemical simulation as a black-box function to find molecules with desired properties (e.g., HOMO/LUMO gap).

## 1.2. Black-Box Optimization

Figure 2 shows the iterative processes of black-box optimization based on ML. For each iteration, the next input is recommended as follows. First, ML is used to predict the black-box function from the data already obtained. When the purpose of optimization is to obtain the highest output, one naive way to make a recommendation is to simply recommend the highest point of the predicted function. However, this approach is known to be suboptimal because of data scarcity.<sup>5</sup> The prediction is never perfect, and there are regions of high uncertainty. Theoretically and practically, it is well-known that the best result is obtained by balancing the predicted function value and uncertainty; that is, the recommended point should have good prediction and high uncertainty at the same time. Such balancing is known as the exploration/exploitation trade-off in the ML community.<sup>6</sup>

## 1.3. Purpose and Structure of This Account

For successful black-box optimization, one needs to select an appropriate algorithm to fit a given problem. In this Account, we introduce various algorithms of black-box optimization in chemistry and materials science in Section 2, together with their applications, as summarized in Table 1. From the viewpoint of information science, each subsection is a mixture of methodologies and concrete algorithms (or implementations), but each subsection basically introduces one method. Although there is a general flow in Section 2, each subsection is independent, and therefore the reader can start reading from the part that is of most interest.

We believe that this Account is beneficial for readers as an overview of the emerging field of automated chemical design.

**Table 1. Summary of Algorithms for Black-Box Optimization and Their Applications<sup>a</sup>**

section	search framework and algorithm	target	search space	objective
2.1	Bayesian optimization (BO) <sup>7</sup>	thermal conductivity <sup>8</sup> (S); interface structure <sup>9</sup> (S); crystal structure <sup>10</sup> (S); interfacial thermal conductance <sup>11</sup> (S); thermal emission <sup>11</sup> (SE); fluorescence <sup>12</sup> (E); thermoelectricity <sup>13</sup> (E); Li-ion conductivity <sup>14</sup> (S; E <sup>15</sup> ) <sup>16</sup> ; single-particle analysis <sup>16</sup> (S); pharmaceutical products <sup>17</sup> (S); metamaterial for radiative sky cooling <sup>20</sup> (S)	large	property optimization
2.2	factorization machine based on quantum annealing <sup>21</sup>	binding pose predictions of protein–ligand <sup>22</sup> (S) and protein–protein complexes <sup>23</sup> (S)	very large	property optimization
2.3	best-arm identification <sup>21</sup>	LogP <sup>24</sup> (S); light-harvesting molecule <sup>2</sup> (SE); identification from NMR signal <sup>25</sup> (S); molecular conformation sampling <sup>25</sup> (S)	small	property optimization
2.4	Monte Carlo tree search (MCTS) <sup>6</sup>	crystal structure prediction <sup>27</sup> (S)	large	property optimization
2.5	gray-box optimization: look ahead based on quadratic approximation (LAQA) <sup>27</sup>	construction of phase diagram <sup>28</sup> (E); rotation of F1-ATPase <sup>29</sup> (S)	large	construction of phase diagram
2.6	active learning: uncertainty sampling <sup>3</sup>	Zn–Sn–P film <sup>28</sup> (E); rotation of F1-ATPase <sup>29</sup> (S)	large	automated discovery for exceptional or out-of-trend materials
2.7	boundless objective-free exploration (BLOX) <sup>4</sup>	light-harvesting molecule <sup>4</sup> (SE)	large	

<sup>a</sup>We classified the studies into three categories: (S) simulation only, (SE) designed or optimized by experiment, and (E) designed or optimized by experiments based on search algorithms. In the search space column, large indicates the extent to which possible candidates can be exhaustively computed with simple but low-precision computational evaluation. Very large means that it is impossible to exhaustively evaluate all candidates even with computationally simple evaluation.

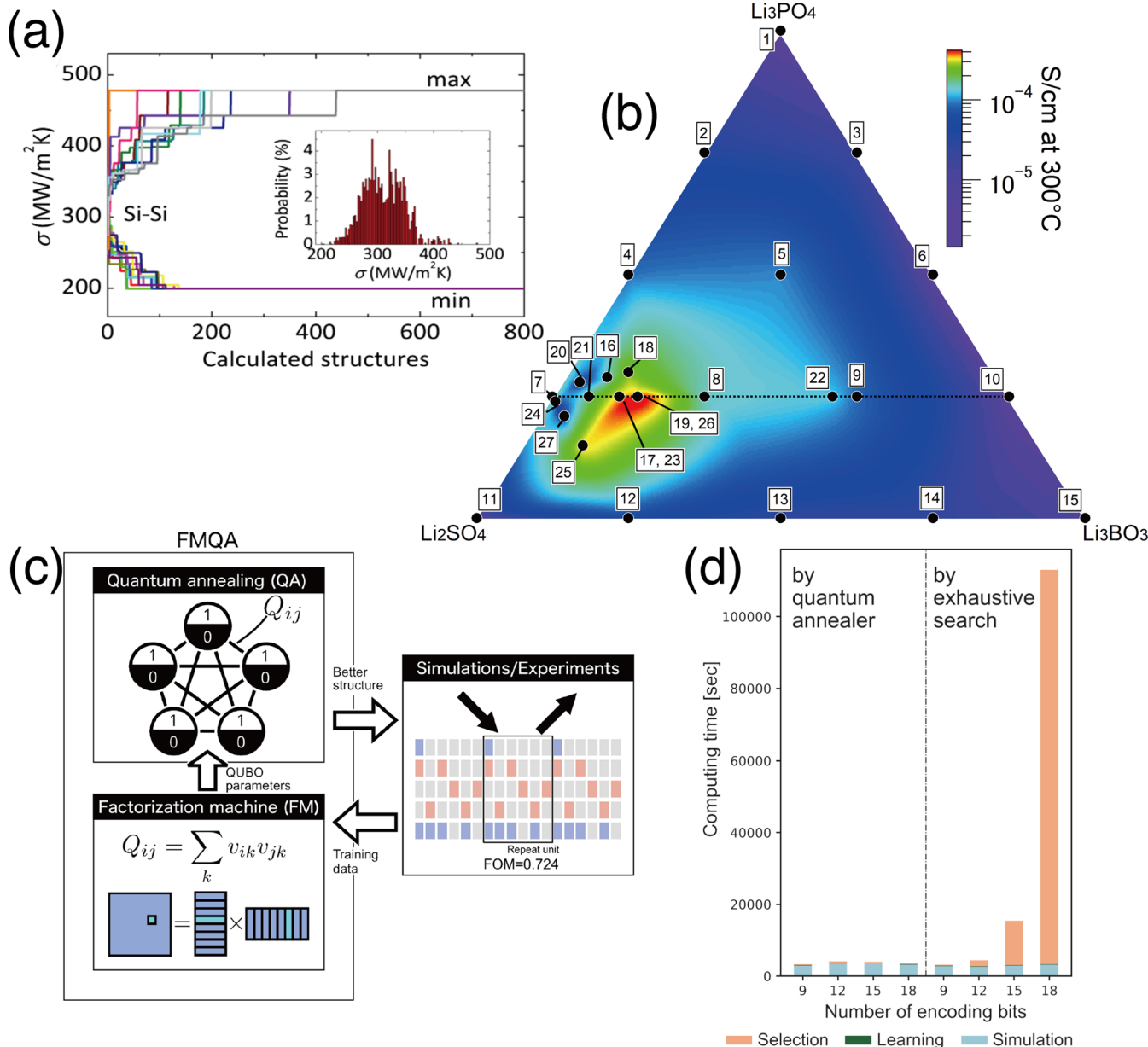


**Figure 3.** Application examples of BO. (a) Some BO runs with different initial choices of candidates to obtain the maximum or minimum ITC. The inset shows the distribution of ITC for all of the candidates. Reproduced with permission from ref 1. Copyright 2017 American Physical Society. (b) Ternary component contour map of Li-ion conductivity by Gaussian process. Points 1–15 are initial data, and the others are recommended by BO. Reproduced with permission from ref 15. Copyright 2020 American Chemical Society. (c) Procedure of black-box optimization with quantum annealing. As a surrogate, FM is adopted, and the selection of the next input is performed by a quantum annealer. (d) Computing time to perform 500 iterations of factorization machine with quantum annealing (FMQA) depending on the problem size with or without D-Wave 2000Q. Panels c and d reproduced with permission from ref 20. Copyright 2020 American Physical Society.

## 2. ALGORITHMS FOR BLACK-BOX OPTIMIZATION AND THEIR APPLICATIONS

### 2.1. Bayesian Optimization

We introduce Bayesian optimization (BO) as a representative algorithm for black-box optimization.<sup>7,30,31</sup> BO uses Gaussian process regression<sup>32</sup> as a surrogate for a black-box function. In this algorithm, first, a regression model that predicts the expected property and variance using Gaussian process is constructed from the already observed input–output pairs. In the case of BO, the expected property and variance based on Gaussian process (GP) correspond to the ML-based prediction in Figure 2b and the uncertainty in Figure 2c, respectively. Here,

the input is the explanatory variable features of materials and molecules, such as compositional ratio, molecular fingerprint, and crystal structure descriptors, and the output is the target property. Next, through the trained regression model, the probable input data that yield the desired output value are also selected by considering the uncertainty of predictions. Then, the true output value for the selected candidate is obtained either through experiments or simulations as black-box functions. BO repeats these processes to find better inputs in the search space. When performing BO, it is necessary to optimize the hyperparameters of the Gaussian process. Our BO library for python, COMBO,<sup>30</sup> provides a function to automatically adjust the hyperparameters by maximization of the type II likelihood,

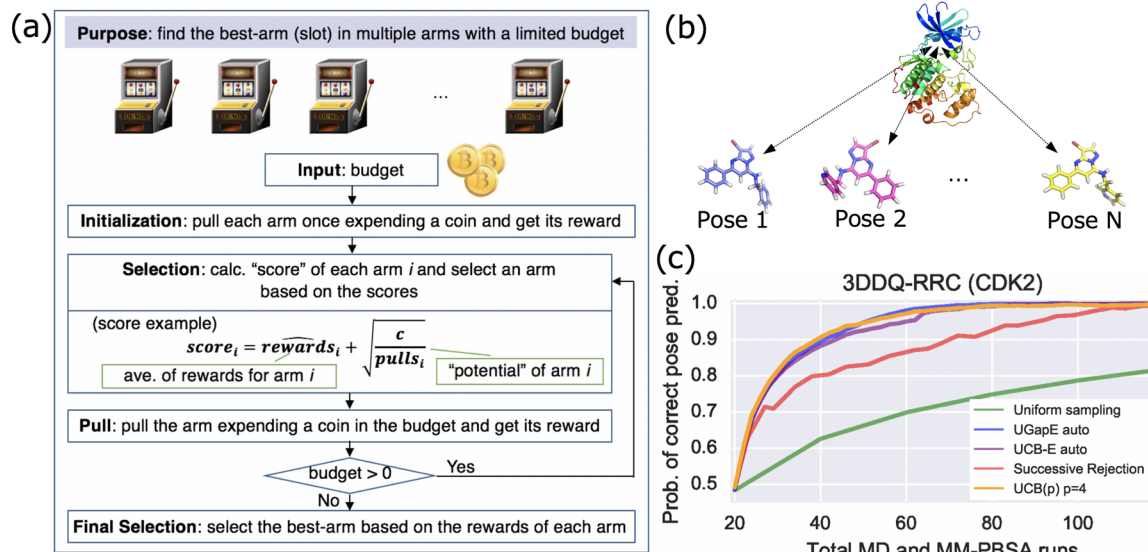


**Figure 4.** (a) Framework of best-arm identification (BAI). The budget means the total number of pulls. (b) Example of binding pose prediction for protein–ligand complexes as a special case of BAI. (c) Effect of BAI algorithms for binding pose prediction of ligand–protein complexes. The computational costs (the number of total binding free energy calculations) were significantly reduced without sacrificing prediction accuracy compared to uniform sampling (green). Panels a and c reproduced with permission from ref 22. Copyright 2018 Oxford University Press.

so that users can use GP and Bayesian optimization without being aware of the hyperparameters.

Many examples of automated discoveries using BO have been reported. For example, we have succeeded in solving black-box optimizations for thermal conductivity,<sup>8</sup> interface structure,<sup>9</sup> crystal structure,<sup>10</sup> interfacial thermal conductance (ITC),<sup>1</sup> thermal emission,<sup>11</sup> fluorescence,<sup>12</sup> thermoelectricity,<sup>13</sup> Li-ion conductivity,<sup>14,15</sup> single-particle analysis,<sup>16</sup> pharmaceutical products,<sup>17</sup> powder manufacturing,<sup>18</sup> and epitaxial TiN thin film.<sup>19</sup> Among them, we choose some examples for a brief review. The first example is optimizing the Si/Ge composite interface structure that minimizes or maximizes ITC. The search space is prepared as arrangements of Si and Ge on 16 sites of the interface structure where the total number of Si and Ge is fixed at 8, respectively. Thus, the total number of candidate structures is 12,870. Here, ITC is calculated using Green's function method. BO can find the optimum structures having the highest or lowest ITC with only a few percent of calculations of ITC against all calculations (see Figure 3a). This research indicates that BO with materials simulations is powerful in nanostructure design for controlling heat conduction. In the second example, the composition of the three mixed materials,  $\text{Li}_3\text{PO}_4\text{-}\text{Li}_3\text{BO}_3\text{-}\text{Li}_2\text{SO}_4$ , is optimized by BO for the purpose of increasing the Li-ion conductivity. In this problem, the search space is the composition ratio with 1% increments of the three materials, and the total number of candidates is 5,151. As initial data, 15 mixing ratios are evaluated and then the optimum mixing composition is successfully found by BO within 6 cycles (see Figure 3b). The found optimum composition is 25 : 14 : 61 ( $\text{Li}_3\text{PO}_4\text{:Li}_3\text{BO}_3\text{:Li}_2\text{SO}_4$  (mol %)), and its Li-ion conductivity was  $4.9 \times 10^{-4}$  S/cm at 300 °C. In this study, experiments are used to obtain properties, and it is shown that BO can accelerate experimental material discovery. Furthermore, the BO method has been improved so that we can use multiple databases with different properties that cannot be integrated in ordinary BO.<sup>33</sup> In this method, the preferences in each database are trained instead of the property value itself. As a demonstration of integration of two databases obtained by simulations, it is shown

that the optimization of absorption wavelength can be accelerated by using a HOMO–LUMO gap database in molecule design. Here, the HOMO–LUMO gap and wavelength are weakly correlated but not directly comparable. Note that our method will integrate some databases having correlation without depending on whether the data are experimental, or computational, or their mixed data.

## 2.2. Factorization Machine with Quantum Annealing

If the search space becomes vast in automated discovery, a combinatorial explosion of candidates for materials and molecules occurs. This explosion often causes a fatal increase in computational time for BO-based recommendations. We have proposed a solution to this problem using the Ising machines, including quantum annealer, which can obtain accurate ground states of the Ising model at high speeds.<sup>20</sup> As a surrogate for a black-box function, the factorization machine (FM), which can be represented by the Ising model, is adopted (Figure 3c). To use FM as a surrogate, it is necessary to express the input of the black-box function by binary variables. Here, finding the minimum condition of the trained FM is equivalent to finding the ground state of the Ising model. In other words, by solving the trained FM with an Ising machine, the next promising candidate can be selected at a high speed from all candidates, and the combinatorial explosion can be avoided. This technique combined with D-Wave quantum annealer (FMQA) is useful for finding the suitable structure of metamaterials for radiative sky cooling.<sup>20</sup> It is shown that the metamaterial structures can be optimized in a short time (Figure 3c), even if the number of candidates is too huge for the ordinary BO to find the better input.

## 2.3. Best-Arm Identification

When a given black-box function is stochastic, i.e., when the result of an experiment or simulation for the same input varies, it is necessary to automatically search for the input that outputs good results stably. In other words, it is required to evaluate the same input multiple times to discover the input with the highest/lowest average of outputs. Here, we introduce the framework of

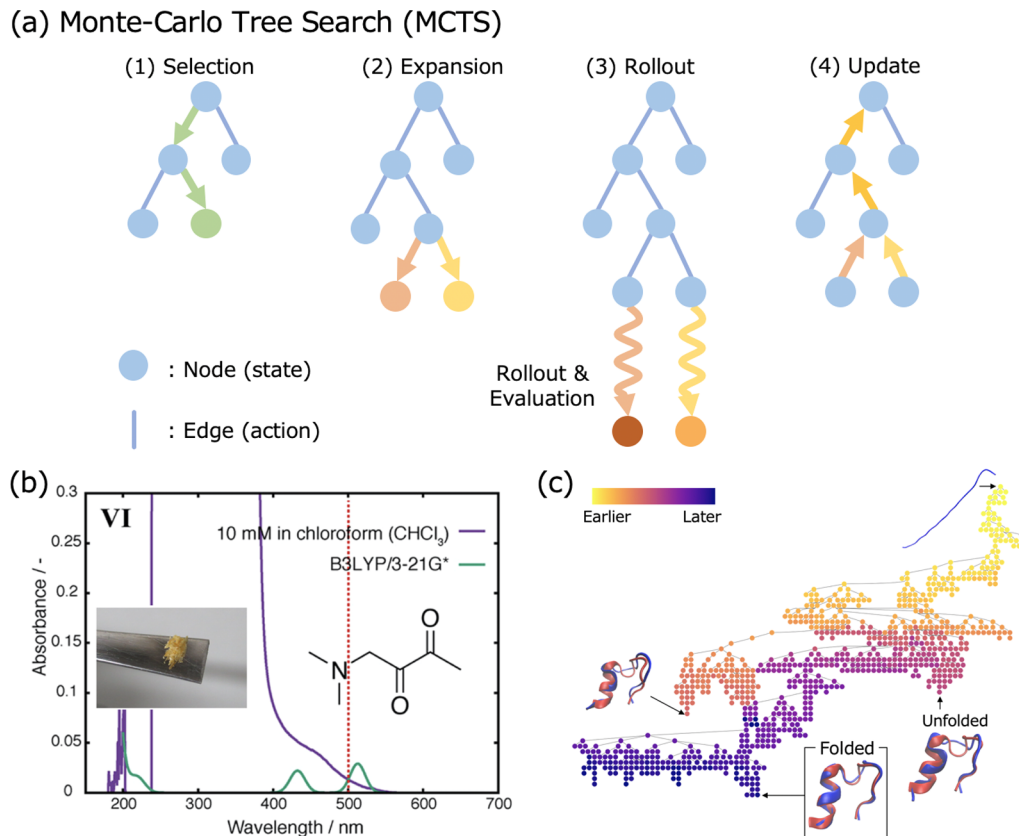


**Figure 5.** (a) Monte Carlo Tree Search (MCTS) algorithm. MCTS repeats procedures 1–4, expanding the search tree. (b) Example of molecules designed by ChemTS<sup>24</sup> coupled with DFT calculations. Adapted with permission from ref 2. Copyright 2018 American Chemical Society. (c) Visualized result of the folding pathway search for Trpcage using the UCT algorithm. Reproduced with permission from ref 26. Copyright 2019 American Chemical Society.

best-arm identification<sup>21</sup> (BAI), a special case of RL,<sup>34</sup> as an effective method in such a black-box optimization situation. BAI is practically used in design of clinical trials<sup>35</sup> and recommendation systems of news.<sup>36</sup> As an application of BAI, we also show that BAI algorithms accelerate binding pose prediction of protein–ligand complexes in computational drug discovery.<sup>22</sup>

BAI is, in short, an exploratory problem to find the most profitable slot machine (called “arm” here) among multiple arms with the smallest number of pulls of their handles, as shown in Figure 4a. Each arm is supposed to return a reward according to its probability distribution. Since we have no information about which arm seems promising at first, we need to pull them widely. On the other hand, we need to concentrate our resources on a few promising arms to identify the best one among them. This is a typical issue of balancing exploration with exploitation for optimal search. Various algorithms<sup>21,37</sup> for solving BAI have been proposed. Here, we introduce upper confidence bound exploration (UCB-E)<sup>21</sup> as a representative example. We first set the total number of times,  $n$ , to pull the arms as a budget. Then, as an initialization, we pull all arms once and obtain their rewards. For each iteration, we calculate the following UCB-E score,  $S_i$ , for each arm  $i$ :

$$S_i = \bar{X}_i + \sqrt{\frac{c}{|X_i|}} \quad (1)$$

and pull the slot with the highest UCB-E score. Here,  $X_i$  is the list of rewards obtained from arm  $i$ ,  $\bar{X}_i$  is the average of the rewards  $X_i$ , and  $|X_i|$  is the total number of pulls for arm  $i$ .  $c$  is a fixed-value parameter that controls the balance between exploration and

exploitation, but it can also be determined automatically during the exploration. Intuitively, the first term contributes to performing exploitation; i.e., the slots with higher average rewards are selected more often, as shown in Figure 2b. On the other hand, the second term is designed to realize exploration based on an evaluation of “uncertainty” corresponding to Figure 2c; that is, the arm with the small number of pulls has high uncertainty. The process of calculating the score and pulling the selected arm is performed  $n$  times. Finally, the arm with the highest average reward is determined to be the best one.

We applied the BAI framework to the problem of binding pose prediction of ligand–protein complexes.<sup>22</sup> This problem can be regarded as selecting the candidate with the lowest binding free energy ( $\Delta G_{\text{bind}}$ ) among several ligand–protein complexes (Figure 4b). Although it is possible to compute approximate  $\Delta G_{\text{bind}}$  through MD simulations and some methods such as the molecular mechanics Poisson–Boltzmann surface area (MM-PBSA) approach as a black-box function, a result of MD simulation depends on its initial condition (velocity/structure). Therefore, to obtain an accurate value of  $\Delta G_{\text{bind}}$ , we need to compute the average of  $\Delta G_{\text{bind}}$ 's, i.e., to perform multiple MD simulations from the same pose candidate. However, multiple MD simulations for all pose candidates require huge computational costs. Here, we can regard this situation as a special case of BAI, considering a pose as an arm and a reward as a  $\Delta G_{\text{bind}}$ . We applied several BAI algorithms to eight protein–ligand complexes and showed that the computational costs (the total number of MD and MM-PBSA calculations) were reduced up to one-fifth, as shown in

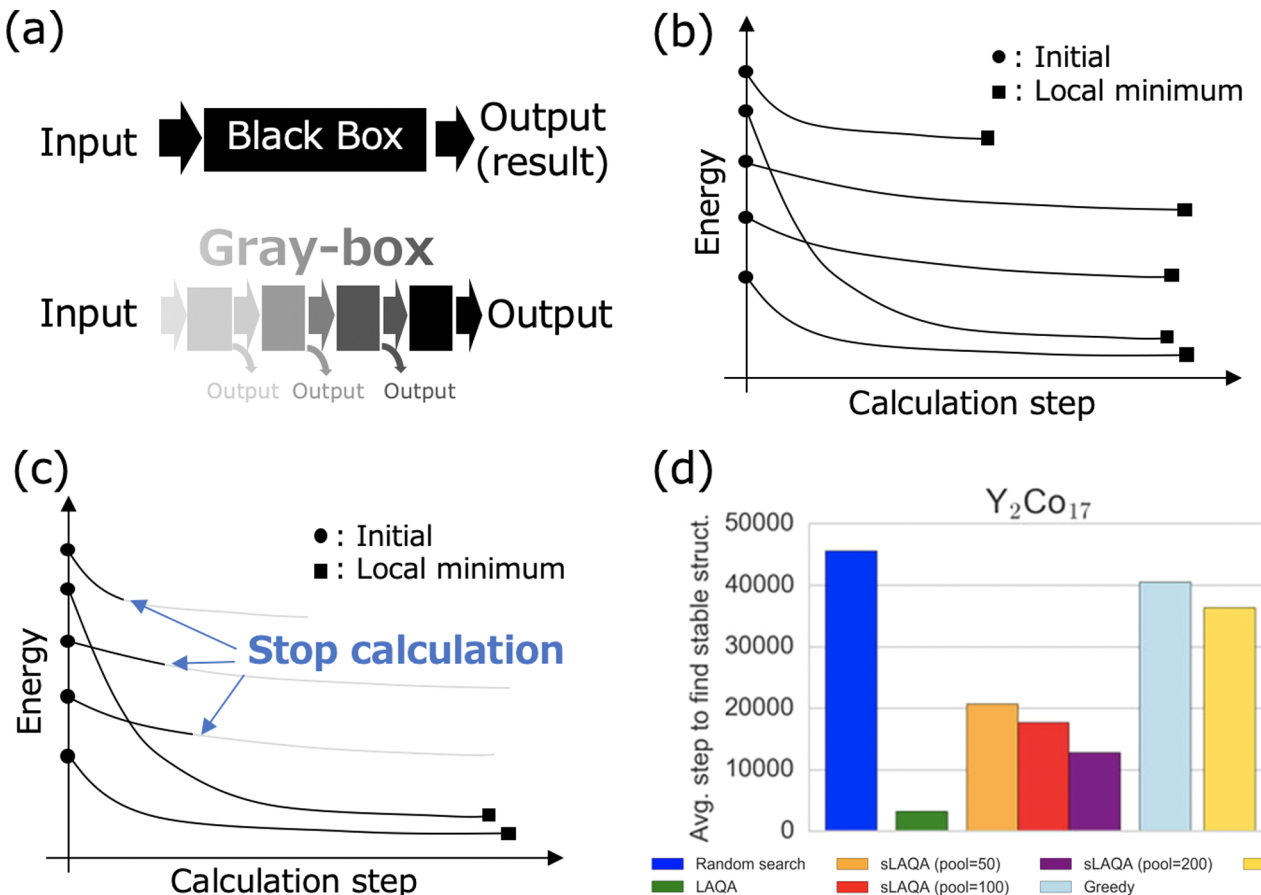


**Figure 6.** (a) Illustration of the black-box and gray-box functions. (b) Schematic diagram of calculation processes for local minimum structures for randomly generated structures in crystal structure prediction. (c) Illustration of the controlling calculation process based on gray-box optimization. (d) Reduction performances of gray-box optimization, including LAQA, compared to random search (blue) for  $\text{Y}_2\text{Co}_{17}$ . Reproduced with permission from ref 27. Copyright 2018 Springer Nature.

Figure 4c. Furthermore, we showed that these BAI algorithms effectively solve a more challenging problem of protein–protein complex structure prediction.<sup>23</sup> In this method, because multiple calculations for each candidate are necessary, the target input space is limited.

#### 2.4. Monte Carlo Tree Search

Here, we introduce examples of black-box optimization using RL, notably the upper confidence bounds for trees (UCT) algorithm and Monte Carlo tree search (MCTS).<sup>6</sup> For example, chemical space consisting of enormous molecules can be treated as the black-box function's input space, as shown in the bottom two examples of Figure 1b. However, the chemical space is too large to prepare all candidate molecules explicitly. Another example of an enormous input space is the possible conformation of a macromolecule, such as a protein. In such situations, reinforcement learning-based algorithms, which can explore in the implicit space while generating required inputs, are often useful.

MCTS is a search algorithm widely used in artificial intelligence (AI) for board games, e.g., AlphaGo,<sup>38</sup> and has recently been used in computer-aided synthesis planning.<sup>39</sup> In MCTS, the search space is represented as a tree structure with nodes and edges, as shown in Figure 5a. Typically, in AI for games, each state in a game is represented as a node in the tree structure and an action from its parent node as an edge. Later, we represent molecules and molecular conformations using this tree

structure. In MCTS, an efficient search is achieved by growing the tree in an appropriate direction by repeating the following procedures (Figure 5a) many times. In procedure 1, we select the location where the node is to be grown on the basis of the previous result using the UCB score, eq. 1, which appeared in BAI. Here, the selection is conducted so that exploration is unbiased, i.e., balancing exploration and exploitation. In procedure 2, the selected node is expanded. Then, in procedure 3, the goodness of the expanded node based on rollout, which means a simulation in some way until the end, and evaluation are calculated. Finally, in procedure 4, the result of the evaluation is reflected in the tree (see Browne et al.<sup>6</sup> for the details of MCTS). Depending on a given problem, various types of searches are possible by preparing nodes and edges to represent the search space and setting up the expansion in procedure 2 and the rollout and evaluation in procedure 3 appropriately.

To discover novel and useful molecules, we proposed a molecule generator, ChemTS,<sup>24</sup> that combines a recurrent neural network (RNN),<sup>40</sup> a type of deep neural network, and MCTS. In ChemTS, a molecule is represented by a SMILES string, and each element of the SMILES string corresponds to a node in a search tree in MCTS. We utilize the RNN-based SMILES character prediction model<sup>41</sup> from an incomplete SMILES string for generating realistic molecules in procedures 2 and 3 in Figure 5a. For designing molecules with a desired property, a molecule generated in procedure 3 needs to be evaluated using the proper criteria. We showed that ChemTS

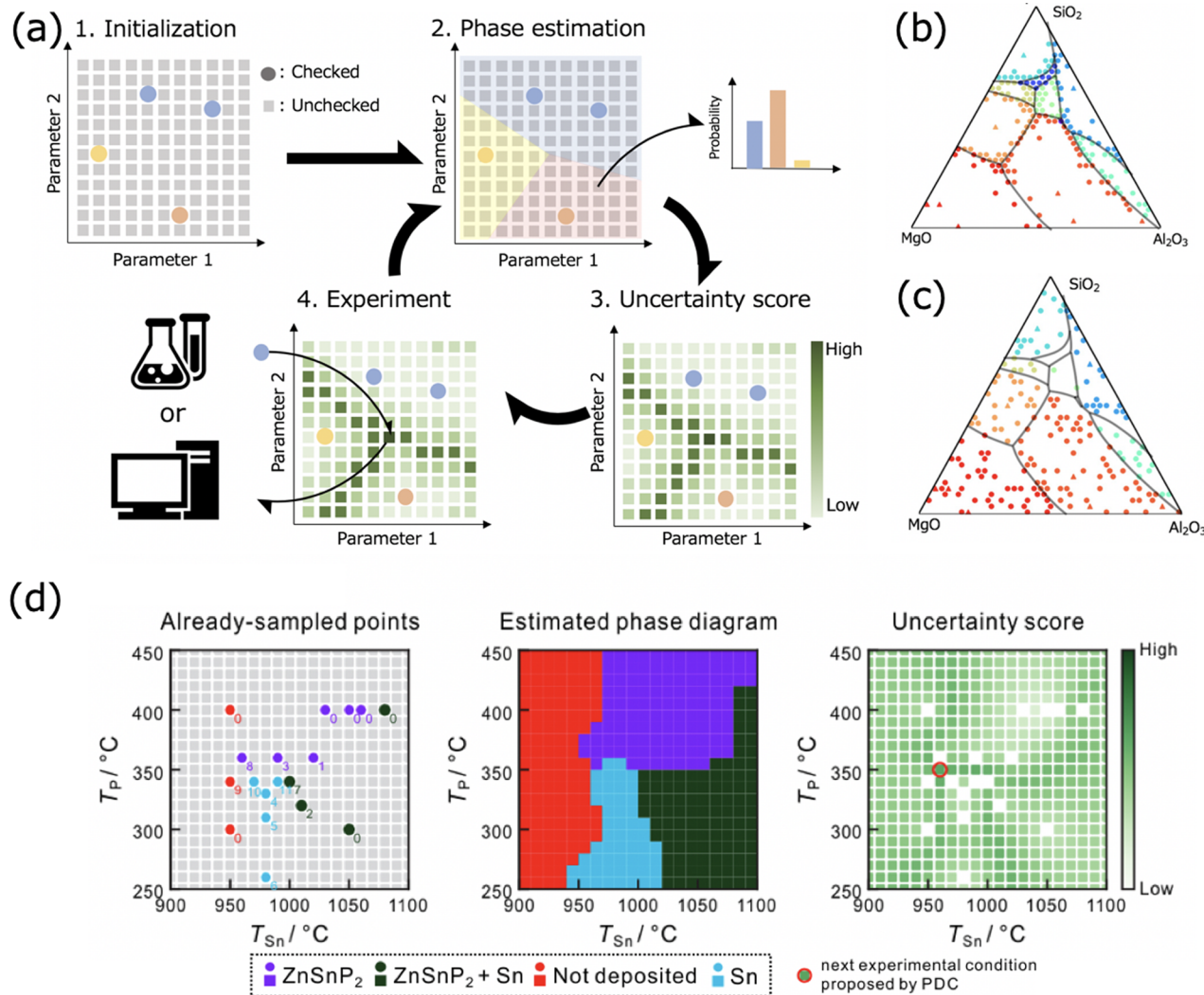


**Figure 7.** (a) Framework of automated phase diagram construction using uncertainty sampling. (b) Points selected by uncertainty sampling for the phase diagram of  $\text{SiO}_2\text{-Al}_2\text{O}_3\text{-MgO}$ . (c) Randomly sampled points for the same diagram in panel b. Panels a–c reproduced with permission from ref 3. Copyright 2019 American Physical Society. (d) Experimentally constructed phase diagram of the deposition of Zn–Sn–P films within 11 cycles using uncertainty sampling. The left, middle, and right parts show the sampled points, estimated phase diagram, and distribution of uncertainty score, respectively. Reproduced with permission from ref 28. Copyright 2020 American Chemical Society.

could effectively generate de novo molecules with high logP values by setting the (black-box) evaluation function of logP in procedure 3.<sup>24</sup>

We have experimentally verified the feasibility of automated molecular design based on ChemTS. We attempted to design molecules with target absorption wavelengths by combining ChemTS and density functional theory (DFT) calculations.<sup>2</sup> We have synthesized six designed molecules and measured their absorption wavelengths (Figure 5b). Although  $\pi\text{-}\pi^*$  excitations are usually controlled in the design of long-wavelength light-harvesting molecules, interestingly, ChemTS has discovered several molecules with  $n\text{-}\pi^*$  excitations at longer absorption wavelengths. This result suggests the possibility of automated discovery of realistic molecules by ChemTS as well as the possibility of unconventional design by AI. ChemTS coupled with electronic simulation such as DFT has high versatility. For example, we have shown that ChemTS can be used for the automatic identification of molecules from  $^1\text{H}$  nuclear magnetic resonance (NMR) spectra without the assistance of chemists.<sup>25</sup>

Tree search algorithms such as MCTS are applicable to the sampling of complex molecular conformations.<sup>26</sup> We utilized the

UCT algorithm, which does not contain the rollout part in MCTS, for protein folding based on MD simulations. We regarded a single conformation as a node in a search tree and short simulations with different initial conditions (velocities) from a node (conformation) as edges from the node. We set the initial state (root node) as an extended structure, the folded structure as a target, and the RMSD for the target as a reward. Figure 5c shows a visualized result of the pathway search for a small protein, Trpcage. The color gradation corresponds to the iterations of the search. As the search progresses, the searched structure gradually approaches the target structure, but it can be trapped in metastable structures, as shown in the unfolded structure in Figure 5c. However, due to the characteristics of the UCT algorithm, the search process avoids metastable structures and eventually moves toward the target structure. The UCT algorithm can be applied to efficient explorations of large conformational changes in proteins and chemical reaction pathways by changing the initial and target structures.

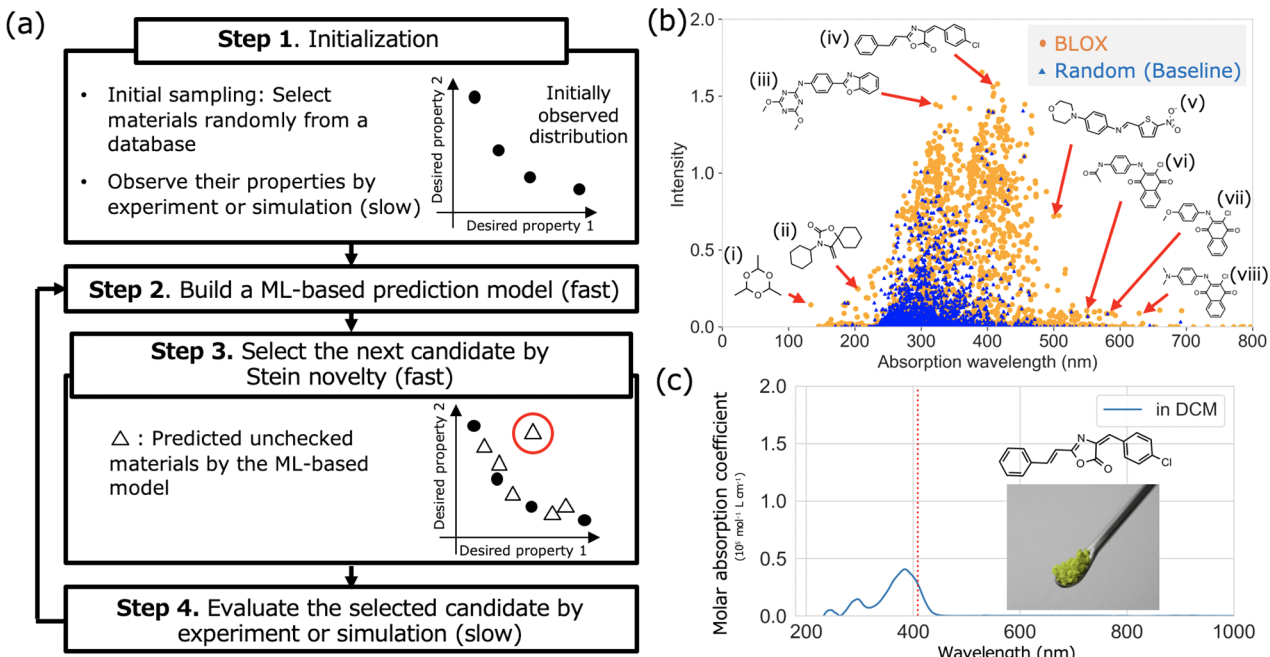


**Figure 8.** (a) Flowchart of boundless objective-free exploration (BLOX) for automated discovery of out-of-trend materials. (b) Sampled 2,000 molecules by BLOX (orange) and random sampling (blue) from the ZINC database. (c) Example of experimental UV–vis absorption spectra of molecule iv in panel and its  $S_1$  energy calculated by DFT (broken red line). Panels a–c reproduced with permission from ref 4. Copyright 2020 Royal Society of Chemistry.

## 2.5. Gray-Box Optimization

Gray-box optimization algorithms<sup>42</sup> are applicable, when we can stop evaluating a black-box function in the middle and estimate the final evaluation value to some extent, as shown in Figure 6a. Gray-box optimization is a framework for efficiently finding the most optimal solution by advancing or stopping the process of computations and experiments. Various algorithms for gray-box optimization<sup>21,37</sup> have been proposed and are used in a hyperparameter search in deep learning. Here, we introduce a gray-box optimization being applied to the crystal structure prediction (CSP) problem.

CSP is a typical example that has a huge search space. Although various methods<sup>43</sup> for CSP have been proposed so far, random search, i.e., a method to search for the most stable structure by generating a large number of input structures at random and finding the local minimum structure around them, is still one of the promising approaches. Figure 6b shows a schematic diagram of the calculation steps to find the local minimum starting from the randomly generated structure. It is possible to utilize the BO framework here,<sup>10</sup> i.e., the input and output of the black-box function are the initial structure and the obtained energy at the local minimum structure, respectively. However, as shown in Figure 6c, we can expect to select promising ones as the calculation proceeds gradually. By stopping the unpromising ones at an early stage and focusing on the promising ones, we can search more efficiently.<sup>37,44</sup> Thus, stopping the calculation to find the local minimum is the reason why this is referred to as a gray box.

We proposed a gray-box optimization algorithm for the CSP problem, named look ahead based on quadratic approximation (LAQA).<sup>27</sup> Although most gray-box optimization algorithms focus on a single score, in the fields of computational chemistry and materials science, it is often possible to obtain not only energy but also its derivatives to atomic positions, such as force and stress. LAQA selects promising candidates and computes

them intensively by roughly approximating each structure's final energy with a quadratic function using energy and force. If a structure has high energy with a small force in the early stage of its calculation process to the local minimum structure, its final energy is expected to be high. Hence, we terminate the calculation process in the early stage. We applied LAQA to the CSP problems of several systems, including Si,  $\text{Al}_2\text{O}_3$ , and ferromagnetic  $\text{Y}_2\text{Co}_{17}$ . The performance of LAQA is 2–20 times faster than that of random search and better than that of BO,<sup>10</sup> as shown in Figure 6d. The gray-box optimization algorithm, including LAQA, is expected to be one of the means of stable structure and molecular conformation searches.

## 2.6. Active Learning

A phase diagram is indispensable in designing materials with desired functionalities. To construct a phase diagram, it is necessary to both determine the phase boundaries and discover new phases efficiently. This situation cannot be directly achieved by the property optimization techniques described above as a black-box optimization problem. Here, we introduce active learning<sup>45</sup> as a different type of black-box optimization from Figure 2 for efficient phase diagrams construction and the discovery of new phases. Active learning is widely used in the field of machine learning to collect training data efficiently.

We utilized uncertainty sampling in active learning for automatically constructing phase diagrams.<sup>3</sup> First, from the information of phases already observed (Figure 7a(1)), we use semisupervised learning to predict the probability distributions of the phases in the input space, where we want to construct a phase diagram (Figure 7a(2)). We then select the input point with the highest “uncertainty” from the estimated probability distribution of the phases (Figure 7a(3)). Various definitions of “uncertainty” have been proposed;<sup>45</sup> for example, the entropy-based approach selects the candidate with the lowest entropy of the probability distribution of the phases. Typically, the points

with high uncertainty scores are distributed around the phase boundaries. The selected point with the uncertainty score is verified experimentally or by simulation as black-box functions (Figure 7a(4)), and the phase data are updated. By repeating these procedures, the phase diagram can be constructed efficiently and automatically.

We applied this framework to the experimentally obtained phase diagrams of  $\text{H}_2\text{O}$  and  $\text{SiO}_2\text{--Al}_2\text{O}_3\text{--MgO}$ .<sup>3</sup> As an example, we show the sampled points by uncertainty sampling and random sampling for the phase diagram of  $\text{SiO}_2\text{--Al}_2\text{O}_3\text{--MgO}$  in Figure 7b,c, respectively. The results showed that the framework succeeded in constructing phase diagrams with approximately one-fifth of the number of samples compared to random sampling, starting from a small number of initial points. Furthermore, as an application to an unreported phase diagram, we applied this framework to the deposition of Zn–Sn–P films by molecular beam epitaxy, which has the potential for metal-free solar cells.<sup>28</sup> As a result, we succeeded in constructing the phase diagram experimentally with discovering new phases within 11 cycles (Figure 7d). In addition, we showed that this framework was also useful for quick identification of successful parameter regions in molecular dynamics simulations of the F1-ATPase motor.<sup>29</sup> Our implementation of active learning for phase diagram construction is available on GitHub at <https://github.com/tsudalab/PDC/> and a representative library of active learning, modal,<sup>46</sup> would also be useful.

## 2.7. Boundless Objective-Free Exploration

If the property's target value to be optimized is fixed, then the methods mentioned above, such as BO, would be useful for automated discovery. However, when there is more than one target property, designing the evaluation function is not always a trivial task.<sup>47,48</sup> Practically, there is a need to discover materials that have optimum multiproperties. Furthermore, useful and unexpected materials can be evaluated by their rareness results in deviation from a trend. Therefore, we proposed a new black-box optimization algorithm, boundless objective-free exploration (BLOX), which combines several machine learning techniques to both characterize the trend in the data and automatically search for exceptional data that deviate from the trends.<sup>4</sup>

Figure 8a shows the search procedure of BLOX. First, we make a set of target properties (step 1). The procedure of the search cycle starts from the construction of a model that predicts properties using the already obtained data based on supervised learning methods (step 2). In the early stages of the search, the accuracy of the model might be low because of the small amount of data, but it is improved as the search progresses. We then use this prediction model to predict the values of the properties for unchecked input candidates. The open triangles in step 3 of Figure 8 show the predicted values of the input candidates. Most outliers from these predicted data are selected using Stein discrepancy,<sup>49</sup> which allows a kind of measurement of the distance between the distribution of data on the property space and the uniform distribution. On the basis of this distance measurement, we can automatically select the unchecked data that deviate from the trends of the data boundlessly. Finally, we verify the selected data by experiments and simulations (black-box functions) and add them to the data (step 4).

As an application of BLOX, we searched for light-harvesting molecules in the ZINC database<sup>50</sup> using DFT calculations. Because ZINC is a database consisting of medical molecules, optical absorption properties have rarely been investigated.

Figure 8b shows the sampled results of 2,000 cycles by BLOX (orange dots) and the randomly sampled 2,000 points (blue dots). The orange dots are distributed broadly. Furthermore, we measured the absorption wavelengths of molecules i–viii in Figure 8b and confirmed that the DFT calculation agrees with the experimental data (Figure 8c). This result indicates that BLOX is an effective tool for automated discovery of out-of-trend materials and chemical repurposing.

## 3. SUMMARY AND OUTLOOK

To meet ever more pressing environmental problems including  $\text{CO}_2$  emission reduction and renewable energy development, new materials have to be discovered at an accelerated speed. To revolutionize how materials are discovered, one needs to improve the productivity of each research scientist and also invite more people to participate in materials discovery. Black-box optimization methods introduced in this Account contribute to both goals. Machine learning would serve as a good companion to a well-educated researcher by offering a means to explore the materials space more efficiently. Perhaps more importantly, machine learning lowers a hurdle for newcomers and democratizes materials development. Typically, materials discovery requires a huge pile of knowledge in physics and chemistry that can only be obtained by education for many years. Although the importance of knowledge should never be understated, machine learning allows less-trained users to get interested in this important field of science, because automated discovery systems work without human knowledge. This attracts start-up companies and academic researchers who have no experience in materials science to start new projects.

In this Account, we introduced various automated discovery algorithms and their applications from the viewpoint of black-box optimization. Our implementations of black-box optimization are summarized in <https://github.com/tsudalab>. The algorithms presented in this Account are by no means exhaustive. We mainly introduced optimization methods for a single property. However, for practical discovery and design, it is often desirable to optimize multiple properties simultaneously, and various multiobjective black-box optimization methods<sup>47,48</sup> are available. In addition, deep learning methods for the generation and design of molecules and materials based on generative models are prominent examples of the latest development.<sup>51</sup> We mainly focused on BAI and MCTS as examples of reinforcement learning in this Account, but various methods such as those combined with deep learning are actively being developed.<sup>52,53</sup> There is no doubt that these algorithms will accelerate scientific discovery and improve the efficiency of materials design.

At present, the biggest bottleneck in automated discovery is laboratory experiments. In several examples in this account, we succeeded in experimentally verifying that molecules and materials optimized on the basis of computations have the properties near to the desired values. However, these experiments are not always successful and require considerable time and money. Hence, it is necessary to develop designing methods for molecules with high synthesizability<sup>54</sup> and materials with high feasibility including cost. In comparison to experiments, simulation techniques such as quantum chemistry calculations create much more data in unit time; hence, automated discovery methods fare better with simulation. In the future, we believe that new algorithms for automated discovery, improvements on simulation techniques in quantum chemistry including first-principles calculations, and the development of laboratory

automation and robotics<sup>55,56</sup> will narrow the gap between experimentation and simulation, and eventually the application range of automated discovery algorithms will be expanded significantly.

## AUTHOR INFORMATION

### Corresponding Author

Koji Tsuda — Graduate School of Frontier Sciences, The University of Tokyo, Kashiwa 277-8561, Japan; Research and Services Division of Materials Data and Integrated System, National Institute for Materials Science, Tsukuba 305-0047, Japan; RIKEN Center for Advanced Intelligence Project, Tokyo 103-0027, Japan;  orcid.org/0000-0002-4288-1606; Email: [tsuda@k.u-tokyo.ac.jp](mailto:tsuda@k.u-tokyo.ac.jp)

### Authors

Kei Terayama — Graduate School of Medical Life Science, Yokohama City University, Tsurumi-ku 230-0045, Japan; RIKEN Center for Advanced Intelligence Project, Tokyo 103-0027, Japan; Medical Sciences Innovation Hub Program, RIKEN, Yokohama 230-0045, Japan; Graduate School of Medicine, Kyoto University, Sakyo-ku 606-8507, Japan;  orcid.org/0000-0003-3914-248X

Masato Sumita — RIKEN Center for Advanced Intelligence Project, Tokyo 103-0027, Japan; International Center for Materials Nanoarchitectonics (WPI-MANA), National Institute for Materials Science, Tsukuba 305-0044, Japan

Ryo Tamura — Graduate School of Frontier Sciences, The University of Tokyo, Kashiwa 277-8561, Japan; International Center for Materials Nanoarchitectonics (WPI-MANA) and Research and Services Division of Materials Data and Integrated System, National Institute for Materials Science, Tsukuba 305-0044, Japan; RIKEN Center for Advanced Intelligence Project, Tokyo 103-0027, Japan;  orcid.org/0000-0002-0349-358X

Complete contact information is available at:

<https://pubs.acs.org/10.1021/acs.accounts.0c00713>

### Notes

The authors declare no competing financial interest.

### Biographies

**Kei Terayama** is Associate Professor at the Graduate School of Medical Life Science, Yokohama City University. He received a Doctor of Human and Environmental Studies degree in 2016 from Kyoto University. His research interests include developing and applying machine learning and computer vision techniques for chemistry, materials sciences, biology, and underwater monitoring.

**Masato Sumita** is Research Scientist at the Center for Advanced Intelligence Project, RIKEN. He received a Doctor of Science in 2008 from the University of Tsukuba. His research interests include quantum chemistry and application of machine learning for chemistry and materials sciences.

**Ryo Tamura** is Senior Researcher at the International Center for Materials Nanoarchitectonics (WPI-MANA), National Institute for Materials Science (NIMS) and the Lecturer at the Graduate School of Frontier Sciences, The University of Tokyo. He has completed his Ph.D. from The University of Tokyo in 2012. He has worked in the fields of materials science and physics.

**Koji Tsuda** is Professor at the Graduate School of Frontier Sciences, The University of Tokyo. He is also Team Leader at RIKEN Center for

Advanced Intelligence Project and Invited Researcher at the National Institute for Materials Science (NIMS). He received a Doctor of Engineering from Kyoto University in 1998. His research interest includes machine learning, bioinformatics, and materials informatics.

## ACKNOWLEDGMENTS

This work is partially supported by a project subsidized by the New Energy and Industrial Technology Development Organization (NEDO) and MEXT as “Priority Issue on Post-K Computer” (Building Innovative Drug Discovery Infrastructure through Functional Control of Biomolecular Systems) and “Program for Promoting Researches on the Supercomputer Fugaku” (MD-driven Precision Medicine). K. Tsuda is supported by NEDO P15009, SIP (Technologies for Smart Bioindustry and Agriculture), Grants JST CREST JPMJCR1502 and JST ERATO JPMJER1903. K. Terayama is supported by AMED under Grant Number JP20nk0101111. R. Tamura is supported by JST CREST JPMJCR17J2 and SIP (“Materials Integration” for Revolutionary Design System of Structural Materials). This research partially used the computational resources of the supercomputer centers of NIMS and RAIDEN of AIP (RIKEN).

## REFERENCES

- (1) Ju, S.; Shiga, T.; Feng, L.; Hou, Z.; Tsuda, K.; Shiomi, J. Designing Nanostructures for Phonon Transport via Bayesian Optimization. *Phys. Rev. X* **2017**, *7*, 021024.
- (2) Sumita, M.; Yang, X.; Ishihara, S.; Tamura, R.; Tsuda, K. Hunting for Organic Molecules with Artificial Intelligence: Molecules Optimized for Desired Excitation Energies. *ACS Cent. Sci.* **2018**, *4*, 1126–1133.
- (3) Terayama, K.; Tamura, R.; Nose, Y.; Hiramatsu, H.; Hosono, H.; Okuno, Y.; Tsuda, K. Efficient construction method for phase diagrams using uncertainty sampling. *Phys. Rev. Materials* **2019**, *3*, 033802.
- (4) Terayama, K.; Sumita, M.; Tamura, R.; Payne, D. T.; Chahal, M. K.; Ishihara, S.; Tsuda, K. Pushing property limits in materials discovery via boundless objective-free exploration. *Chem. Sci.* **2020**, *11*, 5959–5968.
- (5) Jones, D. R.; Schonlau, M.; Welch, W. J. Efficient global optimization of expensive black-box functions. *Journal of Global Optimization* **1998**, *13*, 455–492.
- (6) Browne, C. B.; Powley, E.; Whitehouse, D.; Lucas, S. M.; Cowling, P. I.; Rohlfsen, P.; Tavener, S.; Perez, D.; Samothrakis, S.; Colton, S. A survey of monte carlo tree search methods. *IEEE Transactions on Computational Intelligence and AI in games* **2012**, *4*, 1–43.
- (7) Shahriari, B.; Swersky, K.; Wang, Z.; Adams, R. P.; De Freitas, N. Taking the human out of the loop: A review of Bayesian optimization. *Proc. IEEE* **2016**, *104*, 148–175.
- (8) Seko, A.; Togo, A.; Hayashi, H.; Tsuda, K.; Chaput, L.; Tanaka, I. Prediction of Low-Thermal-Conductivity Compounds with First-Principles Anharmonic Lattice-Dynamics Calculations and Bayesian Optimization. *Phys. Rev. Lett.* **2015**, *115*, 205901.
- (9) Kiyohara, S.; Oda, H.; Tsuda, K.; Mizoguchi, T. Acceleration of stable interface structure searching using a kriging approach. *Jpn. J. Appl. Phys.* **2016**, *55*, 045502.
- (10) Yamashita, T.; Sato, N.; Kino, H.; Miyake, T.; Tsuda, K.; Oguchi, T. Crystal structure prediction accelerated by Bayesian optimization. *Phys. Rev. Materials* **2018**, *2*, 013803.
- (11) Sakurai, A.; Yada, K.; Simomura, T.; Ju, S.; Kashiwagi, M.; Okada, H.; Nagao, T.; Tsuda, K.; Shiomi, J. Ultranarrow-Band Wavelength-Selective Thermal Emission with Aperiodic Multilayered Metamaterials Designed by Bayesian Optimization. *ACS Cent. Sci.* **2019**, *5*, 319–326.
- (12) Saito, Y.; Oikawa, M.; Nakazawa, H.; Niide, T.; Kameda, T.; Tsuda, K.; Umetsu, M. Machine-Learning-Guided Mutagenesis for

- Directed Evolution of Fluorescent Proteins. *ACS Synth. Biol.* **2018**, *7*, 2014–2022.
- (13) Hou, Z.; Takagiwa, Y.; Shinohara, Y.; Xu, Y.; Tsuda, K. Machine-Learning-Assisted Development and Theoretical Consideration for the Al<sub>2</sub>Fe<sub>3</sub>Si<sub>3</sub> Thermoelectric Material. *ACS Appl. Mater. Interfaces* **2019**, *11*, 11545–11554.
- (14) Sumita, M.; Tamura, R.; Homma, K.; Kaneta, C.; Tsuda, K. Li-Ion Conductive Li<sub>3</sub>PO<sub>4</sub>-Li<sub>3</sub>BO<sub>3</sub>-Li<sub>2</sub>SO<sub>4</sub> Mixture: Revision through Density Functional Molecular Dynamics and Machine Learning. *Bull. Chem. Soc. Jpn.* **2019**, *92*, 1100–1106.
- (15) Homma, K.; Liu, Y.; Sumita, M.; Tamura, R.; Fushimi, N.; Iwata, J.; Tsuda, K.; Kaneta, C. Optimization of Heterogeneous Ternary Li<sub>3</sub>PO<sub>4</sub>-Li<sub>3</sub>BO<sub>3</sub>-Li<sub>2</sub>SO<sub>4</sub> Mixture For Li-Ion Conductivity by Machine learning. *J. Phys. Chem. C* **2020**, *124*, 12865–12870.
- (16) Tokuhisa, A.; Kanada, R.; Chiba, S.; Terayama, K.; Isaka, Y.; Ma, B.; Kamiya, N.; Okuno, Y. Coarse-Grained Diffraction Template Matching Model to Retrieve Multiconformational Models for Biomolecule Structures from Noisy Diffraction Patterns. *J. Chem. Inf. Model.* **2020**, *60*, 2803–2818.
- (17) Sano, S.; Kadokami, T.; Tsuda, K.; Kimura, S. Application of Bayesian optimization for pharmaceutical product development. *Journal of Pharmaceutical Innovation* **2020**, *15*, 333–343.
- (18) Tamura, R.; Osada, T.; Minagawa, K.; Kohata, T.; Hirosawa, M.; Tsuda, K.; Kawagishi, K. Machine learning-driven optimization in powder manufacturing of Ni-Co based superalloy. *Mater. Des.* **2021**, *198*, 109290.
- (19) Ohkubo, I.; Hou, Z.; Lee, J.; Aizawa, T.; Lippmaa, M.; Chikyow, T.; Tsuda, K.; Mori, T. Realization of closed-loop optimization of epitaxial titanium nitride thin-film growth via machine learning. *Mater. Today Phys.* **2021**, *16*, 100296.
- (20) Kitai, K.; Guo, J.; Ju, S.; Tanaka, S.; Tsuda, K.; Shiomi, J.; Tamura, R. Designing metamaterials with quantum annealing and factorization machines. *Phys. Rev. Research* **2020**, *2*, 013319.
- (21) Audibert, J.-Y.; Bubeck, S.; Munos, R. Best Arm Identification in Multi-Armed Bandits. *COLT—23rd Conference on Learning Theory*, Haifa, Israel, Jun. 27–29, 2010.
- (22) Terayama, K.; Iwata, H.; Araki, M.; Okuno, Y.; Tsuda, K. Machine learning accelerates MD-based binding pose prediction between ligands and proteins. *Bioinformatics* **2018**, *34*, 770–778.
- (23) Terayama, K.; Shinobu, A.; Tsuda, K.; Takemura, K.; Kitao, A. evERdock BAI: Machine-learning-guided selection of protein-protein complex structure. *J. Chem. Phys.* **2019**, *151*, 215104.
- (24) Yang, X.; Zhang, J.; Yoshizoe, K.; Terayama, K.; Tsuda, K. ChemTS: an efficient python library for de novo molecular generation. *Sci. Technol. Adv. Mater.* **2017**, *18*, 972–976.
- (25) Zhang, J.; Terayama, K.; Sumita, M.; Yoshizoe, K.; Ito, K.; Kikuchi, J.; Tsuda, K. NMR-TS: de novo molecule identification from NMR spectra. *Sci. Technol. Adv. Mater.* **2020**, *21*, 552–561.
- (26) Shin, K.; Tran, D. P.; Takemura, K.; Kitao, A.; Terayama, K.; Tsuda, K. Enhancing Biomolecular Sampling with Reinforcement Learning: A Tree Search Molecular Dynamics Simulation Method. *ACS Omega* **2019**, *4*, 13853–13862.
- (27) Terayama, K.; Yamashita, T.; Oguchi, T.; Tsuda, K. Fine-grained optimization method for crystal structure prediction. *npj Comput. Mater.* **2018**, *4*, 32.
- (28) Katsume, R.; Terayama, K.; Tamura, R.; Nose, Y. Experimental Establishment of Phase Diagrams Guided by Uncertainty Sampling: An Application to the Deposition of Zn-Sn-P Films by Molecular Beam Epitaxy. *ACS Mater. Lett.* **2020**, *2*, 571–575.
- (29) Kanada, R.; Tokuhisa, A.; Tsuda, K.; Okuno, Y.; Terayama, K. Exploring Successful Parameter Region for Coarse-Grained Simulation of Biomolecules by Bayesian Optimization and Active Learning. *Biomolecules* **2020**, *10*, 482.
- (30) Ueno, T.; Rhone, T. D.; Hou, Z.; Mizoguchi, T.; Tsuda, K. COMBO: An efficient Bayesian optimization library for materials science. *Materials Discovery* **2016**, *4*, 18–21.
- (31) Terayama, K.; Tsuda, K.; Tamura, R. Efficient recommendation tool of materials by an executable file based on machine learning. *Jpn. J. Appl. Phys.* **2019**, *58*, 098001.
- (32) Williams, C. K.; Rasmussen, C. E. *Gaussian processes for machine learning*; MIT Press: Cambridge, MA, USA, 2006; Vol. 2, DOI: [10.7551/mitpress/3206.001.0001](https://doi.org/10.7551/mitpress/3206.001.0001).
- (33) Sun, X.; Hou, Z.; Sumita, M.; Ishihara, S.; Tamura, R.; Tsuda, K. Data integration for accelerated materials design via preference learning. *New J. Phys.* **2020**, *22*, 055001.
- (34) Sutton, R. S.; Barto, A. G. *Reinforcement learning: An introduction*; MIT Press: Cambridge, MA, USA, 2018.
- (35) Villar, S. S.; Bowden, J.; Wason, J. Multi-armed bandit models for the optimal design of clinical trials: benefits and challenges. *Statistical science: a review journal of the Institute of Mathematical Statistics* **2015**, *30*, 199.
- (36) Li, L.; Chu, W.; Langford, J.; Schapire, R. E. A contextual-bandit approach to personalized news article recommendation. *Proceedings of the 19th international conference on World Wide Web*, Apr. 26–30, 2010, Raleigh, NC, USA; International World Wide Web Conference Committee (IW3C2): Geneva, Switzerland, 2010; pp 661–670.
- (37) Karnin, Z.; Koren, T.; Somekh, O. Almost optimal exploration in multi-armed bandits Machine Learning. *PMLR* **2013**, *28*, 1238–1246.
- (38) Silver, D.; Huang, A.; Maddison, C. J.; Guez, A.; Sifre, L.; Van Den Driessche, G.; Schrittwieser, J.; Antonoglou, I.; Panneershelvam, V.; Lanctot, M.; Dieleman, S.; Grewe, D.; Nham, J.; Kalchbrenner, N.; Sutskever, I.; Lillicrap, T.; Leach, M.; Kavukcuoglu, K.; Graepel, T.; Hassabis, D. Mastering the game of Go with deep neural networks and tree search. *Nature* **2016**, *529*, 484–489.
- (39) Segler, M. H.; Preuss, M.; Waller, M. P. Planning chemical syntheses with deep neural networks and symbolic AI. *Nature* **2018**, *555*, 604–610.
- (40) Cho, K.; van Merriënboer, B.; Gulcehre, C.; Bahdanau, D.; Bougares, F.; Schwenk, H.; Bengio, Y. Learning phrase representations using RNN encoder-decoder for statistical machine translation. *arXiv Preprint (Computer Science: Computation and Language)*, Jun. 3, 2014. arXiv:1406.1078. <https://arxiv.org/abs/1406.1078> (accessed Nov 5, 2018).
- (41) Segler, M. H. S.; Kogej, T.; Tyrchan, C.; Waller, M. P. Generating Focused Molecule Libraries for Drug Discovery with Recurrent Neural Networks. *ACS Cent. Sci.* **2018**, *4*, 120–131.
- (42) Feurer, M.; Hutter, F. Hyperparameter Optimization. In *Automated Machine Learning: Methods, Systems, Challenges*; Hutter, F., Kotthoff, L., Vanschoren, J., Eds.; Springer International: Cham, Switzerland, 2019; pp 3–33, DOI: [10.1007/978-3-030-05318-5\\_1](https://doi.org/10.1007/978-3-030-05318-5_1).
- (43) Oganov, A. R., Ed. *Modern methods of crystal structure prediction*; John Wiley & Sons, 2011; DOI: [10.1002/9783527632831](https://doi.org/10.1002/9783527632831).
- (44) Domhan, T.; Springenberg, J. T.; Hutter, F. Speeding up automatic hyperparameter optimization of deep neural networks by extrapolation of learning curves. *IJCAI'15: Proceedings of the 24th International Joint Conference on Artificial Intelligence*; AAAI Press: Palo Alto, CA, USA, 2015; pp 3460–3468.
- (45) Settles, B. *Active learning literature survey*; Department of Computer Sciences, University of Wisconsin: Madison, WI, USA, 2009.
- (46) Danka, T.; Horvath, P. modAL: A modular active learning framework for Python. *arXiv Preprint (Computer Science: Machine Learning)*, May 2, 2018. arXiv:1805.00979. <https://arxiv.org/abs/1805.00979> (accessed Nov 3, 2018).
- (47) Winter, R.; Montanari, F.; Steffen, A.; Briem, H.; Noé, F.; Clevert, D.-A. Efficient multi-objective molecular optimization in a continuous latent space. *Chem. Sci.* **2019**, *10*, 8016–8024.
- (48) Clancy, P. Balancing Multiple Goals and Making It Work for Materials Research. *ACS Cent. Sci.* **2020**, *6*, 464–466.
- (49) Liu, Q.; Lee, J.; Jordan, M. A Kernelized Stein Discrepancy for Goodness-of-fit Tests. *Proceedings of the 33rd International Conference on Machine Learning*, Jun. 20–22, 2016, New York, New York, USA Journal of Machine Learning Research (JMLR), 2016; Vol. 48, pp 276–284.
- (50) Sterling, T.; Irwin, J. J. ZINC 15 - Ligand Discovery for Everyone. *J. Chem. Inf. Model.* **2015**, *55*, 2324–2337.
- (51) Sanchez-Lengeling, B.; Aspuru-Guzik, A. Inverse molecular design using machine learning: Generative models for matter engineering. *Science* **2018**, *361*, 360–365.

(52) Zhou, Z.; Kearnes, S.; Li, L.; Zare, R. N.; Riley, P. Optimization of molecules via deep reinforcement learning. *Sci. Rep.* **2019**, *9*, 10752.

(53) Gottipati, S. K.; Sattarov, B.; Niu, S.; Pathak, Y.; Wei, H.; Liu, S.; Thomas, K. M. J.; Blackburn, S.; Coley, C. W.; Tang, J.; Chandar, S.; Bengio, Y. Learning To Navigate The Synthetically Accessible Chemical Space Using Reinforcement Learning. *arXiv Preprint (Computer Science: Machine Learning)* Apr. 26, 2020. arXiv:2004.12485. <https://arxiv.org/abs/2004.12485>

(54) Jang, J.; Gu, G. H.; Noh, J.; Kim, J.; Jung, Y. Structure-Based Synthesizability Prediction of Crystals Using Partially Supervised Learning. *J. Am. Chem. Soc.* **2020**, *142*, 18836–18843.

(55) Steiner, S.; Wolf, J.; Glatzel, S.; Andreou, A.; Granda, J. M.; Keenan, G.; Hinkley, T.; Aragon-Camarasa, G.; Kitson, P. J.; Angelone, D.; Cronin, L. Organic synthesis in a modular robotic system driven by a chemical programming language. *Science* **2019**, *363*, eaav2211.

(56) Coley, C. W.; Thomas, D. A.; Lummiss, J. A. M.; Jaworski, J. N.; Breen, C. P.; Schultz, V.; Hart, T.; Fishman, J. S.; Rogers, L.; Gao, H.; Hicklin, R. W.; Plehiers, P. P.; Byington, J.; Piotti, J. S.; Green, W. H.; Hart, A. J.; Jamison, T. F.; Jensen, K. F. A robotic platform for flow synthesis of organic compounds informed by AI planning. *Science* **2019**, *365*, eaax1566.